

Research paper

Development of an efficient vehicle-to-grid method for massive electric vehicle aggregation

Mingyu Seo ^a, Daisuke Kodaira ^b, Yuwei Jin ^a, Hyeongyu Son ^a, Sekyung Han ^{a,*}^a School of Electronic and Electrical Engineering, Kyungpook National University, Daegu 41566, Republic of Korea^b Information and Systems, University of Tsukuba, Tsukuba 305-8573, Japan

ARTICLE INFO

Keywords:

Electric vehicle
Clustered energy storage
Multi-stage optimization
Computation time reduction
Auxiliary services

ABSTRACT

The growing adoption of renewable energy and electric vehicles (EVs) has contributed to environmental sustainability; nevertheless, integration of these products into the power grid has become complex owing to their unpredictable nature and variable energy demands. A significant challenge lies in the realization of large-scale, coordinated control of EVs to serve as an alternative to traditional energy storage systems. This challenge is underscored by the complexity of optimization in large-scale cooperative control problems and the difficulty in reducing such problems to an easily manageable and practical level in real-world application. In response to these challenges, a practical mechanism for the integration of EVs into a vehicle-to-grid concept is proposed in this study. In this approach, the constraints involved in merging multiple EVs into a fictitious clustered energy storage unit, which are often neglected, are given renewed focus. An iterative multi-stage optimization method is introduced that includes an EV aggregation clustering model, multi-tier optimization model, and recursive framework. Here, marked efficacy for larger EV fleets is demonstrated for this method, providing optimal charging and discharging schedules for each vehicle while a high degree of precision is maintained. With the proposed technique, validated through numerous case studies using historical data, the global optimum solution is largely approximated, with a marginal deviation of 4 %. In addition, robustness of the model is demonstrated under varying pricing scenarios, with a computation time that increases in a linear manner, rather than exponentially, as the number of EVs increases. Meanwhile, compared with conventional methods, the technique proposed in this study has the capacity to fulfill the charging demands of all users with reduced charging expense, demonstrating the high precision and efficacy of the technique.

1. Introduction

The transition towards renewable energy sources (RESs) and the rise in electric vehicle (EV) use has marked progress in environmental sustainability but has introduced fluctuations in the power supply due to the intermittent nature of renewables and the variable energy demands of EVs. These fluctuations challenge the grid's stability, necessitating innovative solutions for energy management (Dik et al., 2022). Vehicle-to-grid (V2G) strategies have emerged as a viable solution to this problem. V2G leverages the battery storage of EVs to absorb excess energy during low demand and provide additional power during peak periods, thus serving as a dynamic buffer to stabilize the grid (Khan et al., 2018). Effective V2G scheduling is essential because it addresses the critical need for grid balance in the face of renewable energy variability and EV charging demands, ensuring a more reliable and efficient

energy system (Farhat et al., 2021). However, the successful implementation of V2G requires sophisticated control algorithms that can adapt to the unpredictable behavior of EV users, integrating their individual driving patterns and preferences to optimize the grid's performance (Li et al., 2023).

Moreover, for EVs to function as efficient energy buffers for the power grid, large-scale integration and coordinated control are needed. At specific times, the power grid may face high demand, leading to possible strain. This issue underscores the need for a system that can manage the charging and discharging of EVs, balancing energy supply and demand and maintaining grid stability. However, establishing such a control system would involve substantial technical difficulties, mainly as a result of the high demands of data processing and the need for complex decision-making algorithms to optimize the charging and discharging of potentially tens of thousands of EVs (Patil and Kalkhambkar, 2021). To address these challenges, an aggregator that can centrally

* Corresponding author.

E-mail address: skhan@knu.ac.kr (S. Han).

Nomenclature	
<i>Abbreviations</i>	
BAM	Basic Aggregation Model.
CBS	Cluster-based Scheduler.
CPP	Critical Peak Pricing.
DQN	Deep Q-Network.
EACMEV	Aggregation, Clustering Model.
EV	Electric Vehicle.
FCES	Fictitious Clustered Energy Storage.
FHWA	Federal Highway Administration.
ICUI	Incremental Constraint Update and Iteration.
LMP	Locational Marginal Price.
NP-hard	Non-deterministic Polynomial-time Hardness.
PMF	Probability Mass Functions.
RES	Renewable Energy Source.
RHC	Receding Horizon Control.
SOC	State of Charge.
SOE	State of Energy.
TOU	Time-of-Use.
V2G	Vehicle-to-Grid.
<i>Model expressions and variables</i>	
<i>in</i>	Plug-in time of the EV.
<i>dur</i>	Plug-in duration of the EV.
<i>idx</i>	Charging/discharging instance counter of the EV.
<i>vdx</i>	Index of the EV on a cluster with the same plug-in time and
duration.	
$EV_{in,dur}^{vdx}$	EV with index vdx, at plug-in in, for plug-in duration dur.
$IE_{in,dur}^{vdx}$	initial energy amount.
$CD_{in,dur}^{vdx}$	charging demand.
$P_{in,dur,idx}^{vdx}$	charging/discharging power at plug-in in for plug-in duration dur with index idx.
$CP_{in,dur,idx}^{vdx}$	and $DP_{in,dur,idx}^{vdx}$ $EV_{in,dur}^{vdx}$ max charging (discharging) power.
$SOE_{in,dur,idx}^{vdx}$	$EV_{in,dur}^{vdx}$ state of energy.
$Max.SOE_{in,dur}^{vdx}$	and $Min.SOE_{in,dur}^{vdx}$ $EV_{in,dur}^{vdx}$ max (min) SOE available range.
$n_{in,dur}$	Number of EVs that share the same plug-in time in and the same plug-in duration dur.
FEV_{in}	FEV at plug-in <i>in</i> .
$P_{in,idx}^{vdx}FEV_{in}$	charging/discharging power.
$CP_{in,idx}^{vdx}$	and $DP_{in,idx}^{vdx}$ FEV_{in} max charging(discharging) power.
$IE_{in}^{FEV_{in}}$	initial energy amount.
CD_{in}^{idx}	FEV_{in} charging demand.
$SOE_{in,idx}^{vdx}$	FEV_{in} state of energy.
$Max.SOE_{in}^{idx}$	and $Min.SOE_{in}^{idx}$ FEV_{in} max (min) SOE available range.
X_t	Power supplied to the EV fleet at time <i>t</i> .
D_t	Demand power at time <i>t</i> .
D_{peak}	Peak demand power realized in the past.
M	Maximum schedule horizon.

coordinate and control EVs has been proposed (Zhaoan et al., 2020). Coordinated charging, which can be categorized as centralized or decentralized, has been noted to offer various benefits for system operation such as increased power quality (Karthik et al., 2019), capability for frequency and voltage adjustment (Arias et al., 2018), and stabilization effects (Domínguez-Navarro et al., 2019).

With decentralized control being highlighted, strategies have been developed that provide an optimal charging strategy for a local charging station or individual EV based on real-time electricity pricing. The development of optimal charging strategies for individual EVs has been the subject of numerous studies, employing methods such as cooperative game theory (Zhao et al., 2018) and convex optimization (Wang et al., 2018). Furthermore, strategies have been proposed for stabilizing local power grids, such as an operational strategy based on stochastic game theory aimed at reducing peak power and charging costs for charging stations (Alghamdi et al., 2020). A distributed multiagent EV charging control method using the Nash certification equivalence principle has been developed to mitigate the charging impact on the EV fleet (Park and Moon, 2022), while strategies for managing the energy required to charge stations have been suggested (Zhaoan et al., 2020; Paudel et al., 2022). While decentralized control strategies have been advantageous for individual EVs and local grid management, their potential for broader grid stabilization and resource optimization remains untapped. This gap has led to the proposition of centralized control systems, which aim to expand the scope of optimization across the entire power grid, offering a holistic approach to energy management.

Centralized control entails the aggregation of information from all EVs at a central point, where an aggregator is responsible for devising a suitable charging schedule by considering the grid's technical constraints. Several studies have proposed centralized control strategies to address power system stabilization issues (Diaz-Londono et al., 2020; Kandpal et al., 2022). A day-ahead and real-time strategy for optimally operating plug-in EV charging stations was proposed by Diaz-Londono et al. (2020), using energy from a RES and the power grid. Meanwhile, a day-ahead management strategy was put forth by Kandpal et al. (2022)

that reduces the imbalance by controlling the single-phase charging demand of EVs using V2G power transfer. To solve the grid stabilization issue, various optimization methods have been adopted such as heuristic algorithms and convex optimization, which include linear and quadratic programming. Method based on receding horizon control (RHC) have been implemented to address the control uncertainty inherent in RES linkage or market participation (Jin et al., 2020; Wang et al., 2020; Wu and Sioshansi, 2017). Convex-type optimization methods have been adopted, as the proposed control method relies on the updating of the control schedule at each time step. A probabilistic aggregator optimization model has also been proposed for participation in the day-ahead market based on driving data (Jin et al., 2020). A system for centrally fast charging, applying a Monte Carlo random samples technique and two-level complex algorithm, was presented by Wu and Sioshansi (2017). A probability concept for optimization using a centralized control strategy that considers all EVs was proposed by Wang et al. (2020) (e.g., a centralized control strategy based on probability-based vehicle driving data and RES power generation). Control scheme studies have attempted to address these issues through the implementation of systems that fluctuate in accordance with demand, such as critical peak pricing (CPP), real-time pricing, and time-of-use (TOU) (Zhao et al., 2018). A TOU-based peak-shaving and valley-filling framework was proposed by Liang et al. (2019), while the CPP dynamic decision model was used by Yusuf et al. (2021) to improve the load curve and reduce electricity costs.

While centralized control systems are proposed as a solution for achieving grid stability and resource utilization at a larger scale, they bring their own set of challenges. As the number of EVs increases, so does the number of variables in centralized management, leading to a direct proportionality between the number of EVs and the complexity of the control scheme. Specifically, computational complexity can grow exponentially with the number of EVs. For example, if the schedule duration has *T* time frames with three potential scenarios (i.e., discharge, idle, and charge) for each time frame for a single EV, the size of the solution space is 3^T . The solution space is $3^{T \times n}$ if there are *n* EVs to

be controlled. However, the solution space increases exponentially because the control resolution is normally much higher than three. Therefore, the computational burden grows as the number of target EVs increases, particularly if an objective function is designed with non-deterministic polynomial-time hardness (NP-hard). Addressing these computational demands while developing an effective centralized operating strategy for a massive EV fleet remains a critical challenge that needs to be addressed.

An efficient solution is to cluster EVs and consider them as a fictitious clustered energy storage unit (FCES). A variety of studies have considered a massive EV fleet as a FCES, easily retrieving the charging profile of all EVs in a centralized manner and analyzing the system stability based on the increase in charging load with RES (Khan et al., 2021; Qiu et al., 2022) or daily market bidding (Einaddin and Yazdankhah, 2020; Lopez et al., 2019). In this case, missing orders occur when the charge/discharge power is calculated over time because the constraints of individual EVs, particularly the state-of-charge (SOC), are not considered. Related examples are presented in Section IV-1. A strategy for generating convex optimization-based charging profiles following the conversion of vehicles with the same plug-in time into clusters have been developed by Kandpal et al. (2022), Hashemipour et al. (2021), and Wang et al., (2016, 2017). However, in these studies, a method of determining the charging profile for a limited SOC or idle state was applied, which cannot guarantee global optimum control. Moreover, such a system cannot be used as a V2G service (e.g., building energy management), reducing the justification for aggregation control.

Grouping methods and frameworks have been proposed as method for scheduling large-scale fleets (Rezaeimozafar et al., 2021; Sepetanc and Pandzic, 2021). In this context, an improved k-means clustering algorithm dividing EVs into clusters has been presented (Rezaeimozafar et al., 2021). The EVs in each cluster were converted to a FCES, and a two-step scheduling model of day-ahead and real-time was implemented to reduce electricity costs. In Sepetanc and Pandzic (2021), instead of using the charge/discharge power as a determinant, typically performed in most studies, a model to schedule the SOC level over time was proposed. Such an operating model can be used for both day-ahead scheduling and intraday adjustments based on model predictive control if both charging stations and EV fleets belong to the same company. However, the model was limited by the fact that the FCES schedule could not be appropriately distributed to the individual EVs. Related examples are presented in Section IV-2.

Acknowledging the extensive research in centralized and decentralized control strategies, as well as EV fleet aggregation techniques, it becomes evident that these approaches have foundational limitations. Decentralized control, tailored for individual EVs or localized grids, has not adequately addressed the integral system stability or the maximization of resource utilization at the grid-wide level. By centralized control, a comprehensive perspective is offered, yet challenges in computational efficiency are encountered as the number of EVs grows, leading to practical issues for real-time application. In attempts to simplify management, EV fleet aggregation techniques have been applied to treat numerous EVs as a single energy storage entity; however, individual vehicle constraints like state-of-charge are often overlooked by these techniques, resulting in missed orders and, consequently, suboptimal performance of V2G services.

This study seeks to underscore and address these gaps by presenting an innovative model that not only bolsters the computational efficiency required for the centralized control of large EV fleets but also ensures a near-optimal charging/discharging regimen that abides by the physical constraints of aggregated EVs. The introduction of a two-stage optimization scheme within this model plays a pivotal role in curtailing computational complexity and expanding the operational capacity to manage a larger cohort of EVs efficiently. Furthermore, issues pertaining to the aggregation control of massive EV fleets are analyzed, with methods for overcoming these issues presented. With the proposed model, a near-optimal charge/discharge schedule is produced that

satisfies all physical constraints for clustered EVs. Additionally, the computational complexity is significantly reduced through a two-stage optimization scheme that maximizes the affordable number of EVs. In this study, an earlier study conducted by Jin et al. (2020) in the same laboratory is extended and a novel framework for an EV aggregator is presented, addressing the gap between theory and practice by identifying the technical constraints associated with the integration of EVs into the grid. The aggregator can aggregate the schedulable EVs within its control, providing auxiliary services to the power grid. As EV charging behavior is unpredictable, more accurate future forecasts of EV behavior are constructed based on the probability mass function (PMF). Ultimately, a methodology utilizing the scheduler presented in Jin et al. (2020) to formulate an appropriate charge/discharge schedule for a massive EV fleet in a centralized manner is derived.

The primary contributions of this research can be delineated as follows:

- A method for V2G aggregation, combining individual EVs and the FCES, is formulated. This method significantly contributes to the existing body of knowledge by addressing the computational complexity associated with large-scale EV integration into the power grid, a research gap previously identified.
- A tripartite approach for the generation of optimized EV charging and discharging schedules is presented. With this approach, high precision can be maintained in the management of EV energy, particularly with extensive EV fleets, thereby filling a notable gap in the current literature.
- A solution to the technical conundrum of missing orders during the conversion of a substantial number of EVs to a FCES is provided. This solution contributes to the development of effective strategies for managing the technical complexities inherent in large-scale EV integration, a need that has been identified in previous studies.
- The resilience of the proposed model under dynamic pricing conditions is demonstrated, establishing its practical applicability. This finding is significant as it addresses the need for robust V2G models capable of withstanding real-world market conditions, a gap that has been identified in the existing literature.
- The remainder of this paper is organized as follows. A proposed clustering method, referred to as the EV aggregation clustering model (EACM), is presented in Section II. The multi-stage optimization model and a framework of an iterative method for optimization models are developed in Section III. Specific examples of capacity violations and simulation results are presented in Section IV to verify the efficiency of the proposed method. The same objective function is applied to both the proposed methods and the basic aggregation model (BAM), which simultaneously considers all constraints of individual EVs to compare optimization performance. Finally, the conclusions are presented in Section V.

2. Methodology

2.1. EV aggregation model formulation

To reduce the optimization burden, an aggregation scheme is proposed, referred to as the EACM, in which EVs are first organized and then relevant variables are defined to produce a BAM. Next, EVs with similar characteristics are clustered into a FCES. As previously stated, computational complexity grows exponentially with the number of variables and EVs. Therefore, with fewer target EVs, the optimization complexity of this scheme can be significantly reduced. During the EACM process, EVs with the same “plug-in time” are clustered into an FCES.

Fig. 1 shows an example of a BAM with eight EVs from time slot $t = 1$ to $t = 6$. $EV_{in,dur}^{vdx}$ denotes each EV. For example, EV5 plugs in at $t = 3$, and the plug-in duration comprises 3 continuous time slots. Therefore,

Time slot	1	2	3	4	5	6	...	M	Charging Demand
$EV1(EV_{1,2}^1)$	$P_{1,2,1}^1$	$P_{1,2,2}^1$							$CD_{1,2}^1$
$EV2(EV_{2,3}^1)$	$P_{2,3,1}^1$	$P_{2,3,2}^1$	$P_{2,3,3}^1$						$CD_{2,3}^1$
$EV3(EV_{2,4}^1)$	$P_{2,4,1}^1$	$P_{2,4,2}^1$	$P_{2,4,3}^1$	$P_{2,4,4}^1$					$CD_{2,4}^1$
$EV4(EV_{3,3}^1)$		$P_{3,3,1}^1$	$P_{3,3,2}^1$	$P_{3,3,3}^1$					$CD_{3,3}^1$
$EV5(EV_{3,3}^2)$		$P_{3,3,1}^2$	$P_{3,3,2}^2$	$P_{3,3,3}^2$					$CD_{3,3}^2$
$EV6(EV_{4,3}^1)$		$P_{4,3,1}^1$	$P_{4,3,2}^1$	$P_{4,3,3}^1$					$CD_{4,3}^1$
$EV7(EV_{4,3}^2)$		$P_{4,3,1}^2$	$P_{4,3,2}^2$	$P_{4,3,3}^2$					$CD_{4,3}^2$
$EV8(EV_{4,3}^3)$		$P_{4,3,1}^3$	$P_{4,3,2}^3$	$P_{4,3,3}^3$					$CD_{4,3}^3$
									⋮
Total energy required	X_1	X_2	X_3	X_4	X_5	X_6	...	X_M	$EV_{M,1}^{n_{M,1}} \ni P_{M,1,1}^{n_{M,1}}$

Fig. 1. Example of a basic aggregation model.

the subscripts in and dur both assume the value of 3. $EV5$ has the same plug-in duration as $EV4$; therefore, the superscript vdx of $EV5$ is 2, and $EV_{3,3}^2$ represents $EV5$. Each $EV_{in,dur}^{vdx}$ has a decision variable, $P_{in,dur,idx}^{vdx}$, that represents the amount of charge/discharge power for each time slot over the plug-in duration. The control resolution is 1 h, and the plug-in duration of $EV5$ is 3 h; therefore, the set of decision variables is $\{P_{3,3,1}^2, P_{3,3,2}^2, P_{3,3,3}^2\}$. On the right side of Fig. 1, the charging demand for each $EV_{in,dur}^{vdx}$ before plug-out is specified as $CD_{in,dur}^{vdx}$. For $EV5$, the sum of $\{P_{3,3,1}^2, P_{3,3,2}^2, P_{3,3,3}^2\}$ yields $CD_{3,3}^2$. The control resolution is 1 h; therefore, the sum of the hourly power directly yields the energy. While $P_{in,dur,idx}^{vdx}$ and $CD_{in,dur}^{vdx}$ are defined for each vehicle, the overall output of the aggregator for a specific time slot, t , is represented by the variable X_t . Thus, the sum of the variable P on the same vertical axis is X_t , which is mathematically represented as follows:

$$X_t = \sum_{in=0}^t \sum_{dur=t+1-in}^{M+1-in} \sum_{vdx=1}^{n_{in,dur}} P_{in,dur,t+1-in}^{vdx} \quad (1)$$

Once the EACM is developed with clustered vehicles, clustering EVs with the same plug-in time allows for a reduction in the number of EVs. For example, EV sets $\{EV4, EV5\}$ and $\{EV6, EV7, EV8\}$, shown in Fig. 1, can be clustered into FEV_3 and FEV_4 , respectively (Fig. 2). Each FCES is typically represented as FEV_{in} , which shares the same plug-in time, in . With an FCES, the decision variable $P_{in,dur,idx}^{vdx}$ is reduced to $P_{in,idx}$ as in (2). Similarly, the initial energy of the FCES can be reduced, as in (3). The

clustered EVs of a FCES contain various plug-out times; therefore, the available state of energy (SOE) range and charging demand for a specific time slot must be defined as in (4) and (5), respectively. If the available EVs vary over time, the available SOE range and charging demand may also vary over time. The feasibility of the solution to the problem is impacted if a physically unachievable amount of charge is input into $CD_{in,dur}^{vdx}$ within the plug duration. Thus, to confirm the feasibility of the solution, data preprocessing is required in advance. If the solution is unachievable, $CD_{in,dur}^{vdx}$ is changed to the amount of energy that can be charged within plugs (maximum charging rate \times plug duration).

$$P_{in,idx} = \sum_{dur=1}^{M-in} \sum_{vdx=1}^{n_{in,dur}} P_{in,dur,idx}^{vdx} \quad (2)$$

$$IE_{in} = \sum_{dur=1}^{M-in} \sum_{vdx=1}^{n_{in,dur}} IE_{in,dur}^{vdx} \quad (3)$$

$$Max.SOE_{in}^{idx} = \sum_{dur=1}^{M-in} \sum_{vdx=1}^{n_{in,dur}} Max.SOE_{in,dur}^{vdx} \quad (4)$$

$$Min.SOE_{in}^{idx} = \sum_{dur=1}^{M-in} \sum_{vdx=1}^{n_{in,dur}} Min.SOE_{in,dur}^{vdx} \quad (4)$$

$$CD_m^{idx} = \sum_{dur=1}^{idx} \sum_{vdx=1}^{n_{in,dur}} CD_{in,dur}^{vdx} \quad (5)$$

The number of decision variables is reduced to $M \bullet (M+1)/2$ by the EACM, regardless of the number of participating EVs. Although the complexity of EV scheduling depends on the formulation type (e.g., convex or nonconvex), the required memory and computation time

Reduced vehicles with the same “plug-in time” in BAM									
Time slot	1	2	3	4	5	6	...	M	Charging demand
$FEV_1 \ni \{EV1\}$	$P_{1,1}$	$P_{1,2}$	$P_{1,3}$	$P_{1,4}$	$P_{1,5}$	$P_{1,6}$...	$P_{1,M}$	CD_1
$FEV_2 \ni \{EV2, EV3\}$	$P_{2,1}$	$P_{2,2}$	$P_{2,3}$	$P_{2,4}$	$P_{2,5}$...	$P_{2,M-1}$	CD_2
$FEV_3 \ni \{EV4, EV5\}$	$P_{3,1}$	$P_{3,2}$	$P_{3,3}$	$P_{3,4}$...	$P_{3,M-2}$	CD_3	
$FEV_4 \ni \{EV6, EV7, EV8\}$	$P_{4,1}$	$P_{4,2}$	$P_{4,3}$...	$P_{4,M-3}$	CD_4		
									⋮
Total energy required	X_1	X_2	X_3	X_4	X_5	X_6	...	X_M	$FEV_M \ni P_{M,1}$

Fig. 2. Example of an electric vehicle (EV) aggregation clustering model.

increase exponentially with the number of decision variables. As such, EV scheduling has evolved into an NP-hard problem. FCES scheduling is a polynomial problem because the number of clustered variables in the EACM model is constant. However, the redistribution of the FCES schedule to individual EVs is a challenging problem. Regardless of how complex FCES optimization is, the conditions for individual EVs cannot be fully addressed in the FCES formulation. Hence, optimization is performed with relaxed constraints, and the resulting schedule may not be able to be redistributed to individual EVs owing to the physical constraints of each EV. To address this problem, a multi-stage iterative optimization method is introduced in the following section.

2.2. Stage A: FCES scheduling

A centralized schedule based on the clustering of FCESs in the EACM is determined for a massive EV fleet. This model can be optimized for the target application. The optimization model is composed of three stages. Stage A: FCES scheduling; Stage B: dispatch to the clustered EVs; and Stage C: incremental constraint update and iteration (ICUI) method (Fig. 3).

First, an optional charge/discharge schedule for the FCES can be generated in Stage A. The SOC constraints for individual EVs are not considered when the FCES is scheduled. Therefore, the produced Stage A schedule may not be feasible to be dispatched to the EVs and satisfy all the physical constraints of an individual EV. The produced FCES schedule is then dispatched in Stage B. The scheduling process for the massive EVs ends if dispatch is possible; otherwise, excessively relaxed FCES schedules are derived. Hence, the Stage A constraints must be strengthened. However, the constraints cannot be strengthened without knowledge of the cause for non-dispatch. Therefore, this cause is determined by the ICUI, and the Stage A constraint is strengthened.

In Stage A, an optimal schedule for the FCESs is generated by the optimization model, determining the FEV_{in} values, whereby the total electricity cost of the target system is minimized by the objective function. Additionally, optimization is performed from a system-wide perspective, and the benefit is later shared with the individual EVs. The pricing mechanism adopted here is a typical tariff system, consisting of demand and energy charges. The demand charge cost (C^d) is determined by the contracted power (Q_{cont}) and net peak demand realized during the latest contract period, which is typically one year (Q_{usage}) (Electric Rates Table | KEPCO), as in (6).

$$C^d = \begin{cases} w \times 0.3 \times Q_{cont}, & Q_{usage} < Q_{cont} \times 0.3 \\ w \times Q_{usage}, & Q_{usage} \geq Q_{cont} \times 0.3 \end{cases} \quad (6)$$

where w is determined by the contracted power. Meanwhile, the energy charge cost (C_t^e) is determined using a TOU method. Combining these variables, the objective function for FCES scheduling is defined as follows:

$$\underset{\Xi}{\operatorname{argmin}} \sum_{t=0}^M (X_t \times C_t^e + PL \times C^d) + \sum_{t=0}^M \sum_{idx=1}^t (\delta \bullet P_{in,idx}), \quad \Xi \ni \{P_{in,idx}, PL\} \quad (7)$$

subject to

$$X_t + D_t \leq PL \quad (8)$$

$$D_{peak} \leq PL \quad (9)$$

$$SOE_{in,1} = IE_{in}$$

$$SOE_{in,idx+1} = P_{in,idx} + SOE_{in,idx} \quad (10)$$

$$\text{Min}.SOE_{in} \leq SOE_{in,idx} \leq \text{Max}.SOE_{in} \quad (11)$$

$$\sum_{dur=1}^{M-in} \sum_{vdx=1}^{n_{in,dur}} DP_{in,dur,idx}^{vdx} \leq P_{in,idx} \leq \sum_{dur=1}^{M-in} \sum_{vdx=1}^{n_{in,dur}} CP_{in,dur,idx}^{vdx} \quad (12)$$

$$CD_{in}^{idx} \leq \sum_{idx=1}^t P_{in,idx} \quad (13)$$

The electricity cost imposed on the aggregator is represented by the first term in (7). The overall output of the aggregator at time slot t is given by the variable X_t , as described in (1). The term (1) is expressed for BAM, whereas according to (2), X_t equals the overall output of the EACM. Subsequently, the TOU unit price was multiplied to determine the cost of charging the FCES. Conversely, the demand charge cost is more complicated to deploy. The demand charge cost is determined by the net peak demand realized during the latest contract period. Therefore, a logical function for choosing the peak value should be introduced, yielding a nonconvex problem. To address this problem, a slack variable (PL) was introduced with additional constraints in (8) and (9) that regulate the lower bound of PL to the maximum value of the net demand power. With this scheme, PL can be naturally determined at the peak value, treating the problem as a minimization problem. Battery aging is reduced by the second term as unnecessary charge fluctuations are prevented at battery degradation cost, δ . The constraints in (10) and (11) were used to update the SOE of the FCES during the charging period. The sum of the clustered EVs, as shown in (12), limit the charge/discharge power of the FCES. Constraint (13) sets the minimum hourly charging demand for the FCES. The charge/discharge power of the clustered vehicles determines the FCES charging demand, whose requirements should be set differently each hour as vehicles leave.

2.3. Stage B: dispatch to the clustered EVs

During this phase, the scheduled energy of the FCES in Stage A was dispatched to the clustered EVs as the SOE constraint of each EV was considered. The charging demand of an EV should also be considered at

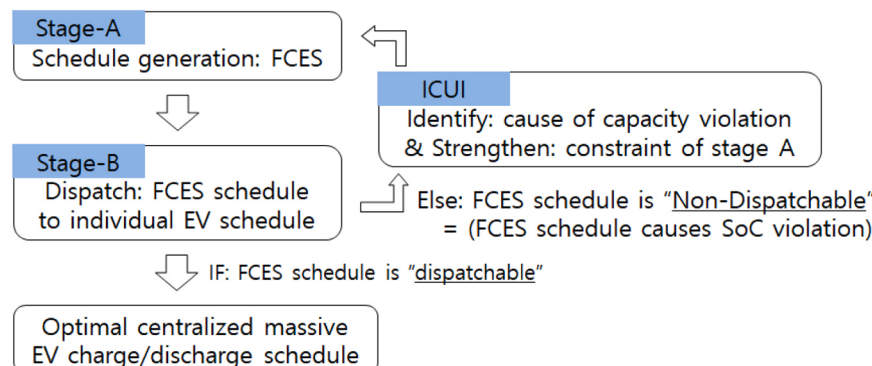


Fig. 3. Multi-stage optimization solution process.

plug-out. Therefore, the objective function is expressed as in (14), considering the time-series argument, $P_{in,dur,idx}^{vdx}$ (i.e., charge/discharge power), for individual EVs. In (14), the unrealized charging demand for each EV is minimized to maximize user convenience. The SOE of individual EVs is updated by the constraints in (15) and (16), whereas the EV power within the charger capacity is regulated in (17). By constraint (18), the total power dispatched to EVs is ensured to be equal to the corresponding FCES power at each time instance.

$$\underset{\Pi}{\operatorname{argmin}} \sum_{in=0}^M \sum_{dur=1}^{M-in} \sum_{vdx=1}^{n_{in,dur}} \left\| CD_{in,dur}^{vdx} - \sum_{idx=1}^{dur} P_{in,dur,idx}^{vdx} \right\|_2, \Pi \\ \ni \left\{ P_{in,dur,idx}^{vdx} \right\} \quad (14)$$

subject to

$$\text{SOE}_{in,dur,1}^{vdx} = \text{IE}_{in,dur}^{vdx}$$

$$\text{SOE}_{in,dur,idx+1}^{vdx} = P_{in,dur,idx}^{vdx} + \text{SOE}_{in,dur,idx}^{vdx} \quad (15)$$

$$\text{Min.SOE}_{in,dur}^{vdx} \leq \text{SOE}_{in,dur}^{vdx} \leq \text{Max.SOE}_{in,dur}^{vdx} \quad (16)$$

$$DP_{in,dur,idx}^{vdx} \leq P_{in,dur,idx}^{vdx} \leq CP_{in,dur,idx}^{vdx} \quad (17)$$

$$\sum_{dur=1}^{M+1-in} \sum_{vdx=1}^{n_{in,dur}} P_{in,dur,idx}^{vdx} = P_{in,dur} \quad (18)$$

2.4. ICUI method

Although the FCES power is limited to the sum of the powers of the clustered EVs, as in (10), it can also be restricted by the SOE level of the individual EVs. However, because the SOE of the individual EV is not considered during FCES scheduling, Stage A might produce an infeasible dispatch schedule for the actual EVs. A specific example of this situation is illustrated in Section IV. Theoretically, this problem can be resolved by deploying all variables for individual EVs in the optimization process. However, as previously discussed, the complexity and computational burden increase exponentially with an increase in the number of EVs, rendering the problem intractable. Thus, partially inspired by the outer approximation method, the ICUI method was proposed (Duran and Grossmann, 1986).

An intuitive analogy of the ICUI method using a navigation problem is presented in Fig. 4. The navigation from start to end has a relaxed condition, binding the optimization complexity, which is analogous to performing Stage A of the FCES schedule without considering the SOE constraints for individual EVs. Then, the feasibility of the derived route corresponding to Stage B is verified. If the route is infeasible (i.e., failure to dispatch to the individual EVs), the obstacle responsible is identified and reflected on the map. Constraints causing energy infeasibility are gradually appended. Then, Stage B is repeated until a detour is successfully found (i.e., Stage B succeeds in distributing the FCES energy to individual EVs). Because the corrected detour may not be optimal from a global route perspective, the entire navigation is re-performed after determining the effect of the obstacle (i.e., rerun Stage A after reflecting the new energy constraint derived in Stage B). A feasibility check is also conducted. This process is repeated until the navigation reaches a feasible route. Similarly, the ICUI process is repeated until the FCES schedule derived in Stage A is successfully dispatched to individual EVs in Stage B.

The structure of the ICUI, comprising three phases, is shown in Fig. 5. During Phase (A), the optimal schedule of the FCES is generated, after which Stage B is used to distribute energy to the clustered EVs. If a feasible solution is found in Stage B, the ICUI process is terminated with the schedules for each EV. Conversely, if a feasible solution is not found, the reason for the infeasibility is identified in Phase (B). Stage B is then rerun after eliminating the SOE constraints of each EV, yielding a tractable problem (problem relaxation). However, owing to relaxation, unrealistic SOE values may be included in the derived solution, such as negative values or values greater than the battery capacity. To curb these capacity violations, a new constraint is created and appended in Stage B, as in (19) where $\text{pre}P_{in,dur,t}^{vdx}$ denotes the amount of charge/discharge in Stage B from the previous iteration as the SOE constraint is added to the relaxed Stage B constraints. Meanwhile, the time step at which the capacity violation occurs in the relaxed Stage B is denoted by Z. This constraint limits the total amount of EV power in the preceding violation. For example, if the SOE of an EV yield is -5 kWh at $t = 3$ and the charging schedule is $\{10 \text{ kW}, -30 \text{ kW} \text{ for } t = 1-2\}$, a constraint of $(P1 + P2) \geq (10-30) - (-5)$ is added to Stage B for the next iteration, limiting the total power in the preceding time to a value smaller than that of the previous one as much as the amount of violation (-5 kW). With this constraint, the possibility of capacity violation is mitigated by limiting the amount of charging power in the preceding period. This

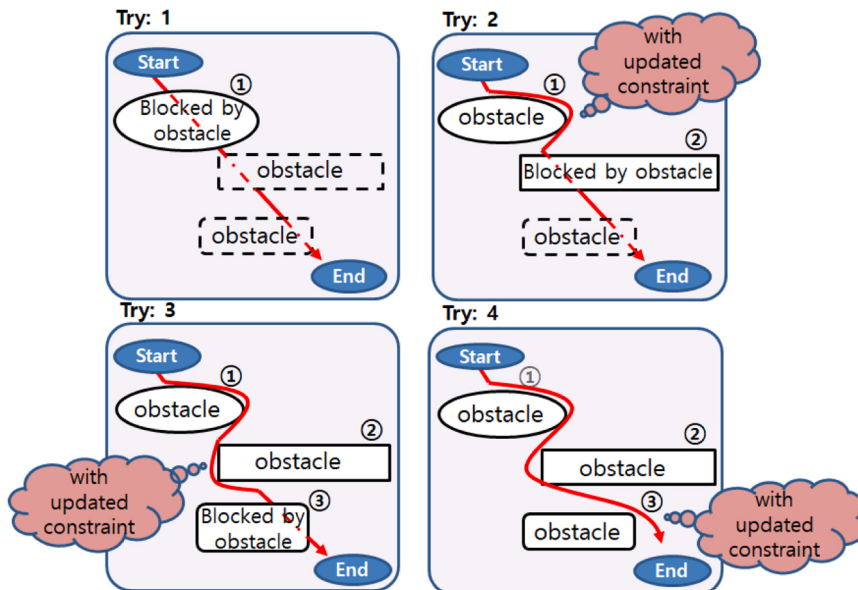


Fig. 4. Navigation analogy for the incremental constraint update and iteration method.

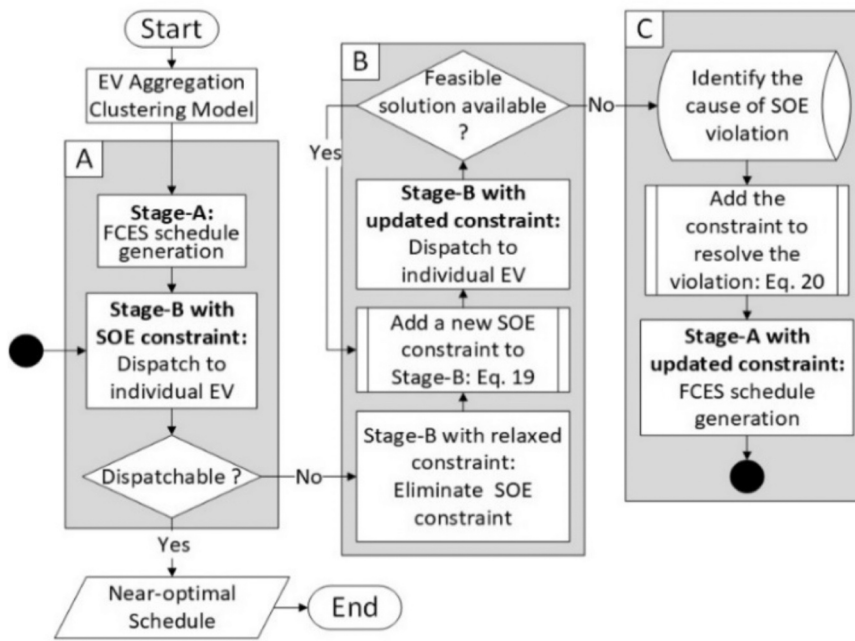


Fig. 5. Workflow of the incremental constraint update and iteration method.

procedure is repeated as new constraints are incrementally appended, until Stage B fails to yield a feasible solution. During Phase (C), the failure of Stage B indicates that the appended constraints have sufficiently re-strengthened the relaxed condition, whereby a critical constraint that was used in the previous iteration causes infeasibility. The FCES schedule in Stage A theoretically causes infeasibility; thus, the critical constraint is then reformed and applied in Stage A, as in (20) where $preP_{in,t}$ denotes the amount of charge/discharge in Stage A from the previous iteration as the constraint of Stage A is strengthened. Once the constraint has been updated, the ICUI returns to Phase (A) and the entire procedure is iterated until a dispatchable FCES schedule is obtained.

$$\text{If : } SOE_{in,dur,Z}^{vdx} > \text{Max.SOE}_{in,dur}^{vdx}$$

$$\sum_{t=1}^{Z-1} \left(P_{in,dur,t}^{vdx} \right) \leq \sum_{t=1}^{Z-1} \left(preP_{in,dur,t}^{vdx} \right) - \left(SOE_{in,dur,Z}^{vdx} - \text{Max.SOE}_{in,dur}^{vdx} \right)$$

Else : $SOE_{in,dur,Z}^{vdx} < \text{Min.SOE}_{in,dur}^{vdx}$

$$\sum_{t=1}^{Z-1} \left(P_{in,dur,t}^{vdx} \right) \geq \sum_{t=1}^{Z-1} \left(preP_{in,dur,t}^{vdx} \right) - \left(SOE_{in,dur,Z}^{vdx} - \text{Min.SOE}_{in,dur}^{vdx} \right) \quad (19)$$

$$\text{If : } SOE_{in,Z} > \text{Max.SOE}_{in}$$

$$\sum_{t=1}^{Z-1} P_{in,t} \leq \sum_{t=1}^{Z-1} preP_{in,t} - \left(SOE_{in,Z} - \text{Max.SOE}_{in} \right)$$

Else : $SOE_{in,Z} < \text{Min.SOE}_{in}$

$$\sum_{t=1}^{Z-1} P_{in,t} \geq \sum_{t=1}^{Z-1} preP_{in,t} - \left(SOE_{in,Z} - \text{Min.SOE}_{in} \right) \quad (20)$$

3. Results and discussion

An EV fleet can be considered an FCES in two schemes: (1) EV similarity and (2) SOC level. In both schemes, the missing order occurs in different forms. For a clear understanding, each issue was analyzed based on specific examples presented in Cases 1 and 2. In Case 1, the problem of Scheme 1 is considered and ICUI is presented as a solution. In Case 2, the problem of Scheme 2 is presented and compared with the ICUI. Finally, the optimality and scalability of the proposed centralized

massive EV control method are verified and compared with the global optimal solution for quantitative performance verification.

In this study, a diverse range of EVs were considered, categorized by type and battery capacity. A total of 18 different electric vehicle models were included, with their battery capacities listed in Table 1 (Jin et al., 2020). Building upon our own previous research conducted in the same lab (Jin et al., 2020), data from the U.S. Federal Highway Administration (FHWA) were utilized to construct PMFs that encapsulate EV charging behavior. This includes variables such as parking time, plug-in time, and initial SOC, graphically represented in Figs. 6 and 7. These PMFs were subsequently employed in Monte Carlo simulations to estimate the charging behavior of each EV within the EV aggregator.

To ensure real-time applicability of our optimization model, we incorporated the concept of RHC into our methodology. This strategy, also utilized in our previous work (Jin et al., 2020), enables real-time control by perpetually updating the optimization model with the most recent data. This approach guarantees that our model can adapt to changes in real-world scenarios, enhancing its practical applicability. The effectiveness of RHC in managing control uncertainty is

Table 1
Electric vehicle information.

Brand	Model	Battery capacity (kWh)	Brand sales Rate (%)
Mi	i-MiEV	16	0.23
Smart	ED	17.3	1.18
Chevrolet	Spark EV	18.3	1.19
Honda	FIT	20	0.16
Fiat	500e	24	4.28
Honda	Clarity	25.5	0.33
BMW	i3	27.2	5.98
Mercedes	B250e	28	0.68
Ford	Focus-e	33.5	1.38
VW	e-Golf	35.7	2.16
Hyundai	Ioniq-e	38.3	0.13
Nissan	LEAF	40	17.73
Toyota	RAV4	41.8	0.37
Chevrolet	Bolt EV	60	6.75
Kia	Soul EV	64	1.03
Tesla	Model 3	78	22.8
Tesla	Model S	100	23.02
Tesla	Model X	100	10.6

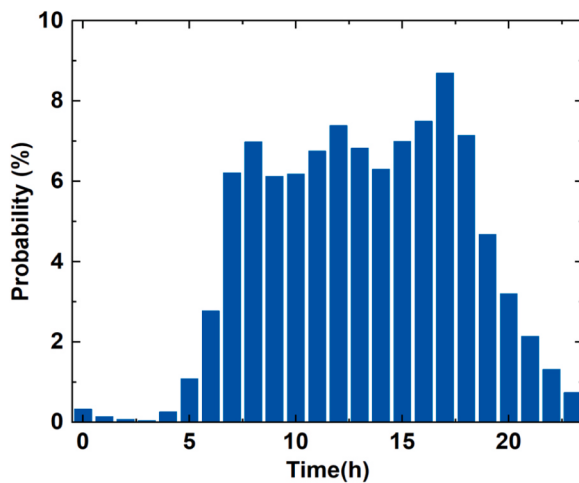


Fig. 6. Hourly plug-in time probability mass function.

well-documented in several studies, including those focused on power system stabilization and RES linkage. For instance, a robust stabilization strategy for a networked microgrid system with uncertainty has been proposed (Khalil et al., 2023). In this strategy, a master-slave control architecture and the Hoo control problem are leveraged, using the Lyapunov-Krasovskii functional to develop a stability criterion in the form of a bilinear matrix inequality. A gray wolf optimizer is used to minimize the performance index and derive the stabilizing controller. Through this approach, the uncertainty in microgrid energy management is effectively addressed, demonstrating the practical applicability and effectiveness of RHC in real-world scenarios. A schematic diagram of the RHC approach is provided in Fig. 8 to further illustrate this concept.

3.1. Case 1: individual EV condition issues omitted in FCES

When the FCES is scheduled, the SOC constraints for the individual EVs are not considered. Therefore, the resulting schedule of various FCES scheduling methods, including Stage A and that provided by Rezaeimozafar et al. (2021), may not be feasible for dispatch to the relevant EVs. The reasons and method for dispatching the FCES schedule are discussed in Case 1. The configurations of the three EVs comprising the FCES are listed in Table 2 as an example.

For simplicity, the plug-in period, battery capacity, and target SOE of each EV assumed identical values. The TOU price for $t = 1-11$ h is represented by the blue line in Fig. 9(a), while the charging/discharging schedule of the FCES by time slot, derived from Stage A based on the specifications in Table 2 and TOU, is represented by the black line. The expected SOE of the FCES is depicted in Fig. 9(b) according to the FCES schedule. As Stage A was designed to minimize the energy cost, the FCES was scheduled to deplete its initial SOE of 85 kWh during the on-peak period ($t = 1-4$) in Stage A, with an even discharge power of 21.25 kW (Fig. 9(a)). This value should not be a problem for the FCES as the discharge power limit of the FCES was 30 kW and the initial SOE was 85 kWh. Both are affordable values from an FCES perspective (Fig. 9(b)).

However, regardless of how the discharge schedules for the EVs were

Table 2
Electric vehicle configuration for Case 1.

Parameters	EV1	EV2	EV3	FCES
Battery capacity [kWh]	50	50	50	150
Initial energy [kWh]	50	30	5	85
Target SOE [kWh]	50	50	50	150
Charging demand [kWh]	0	20	45	65
Charge/Discharge power limit [kW/h]	10/-10	10/-10	10/-10	30/-30
Plug-in time	$t = 1 - 11$			

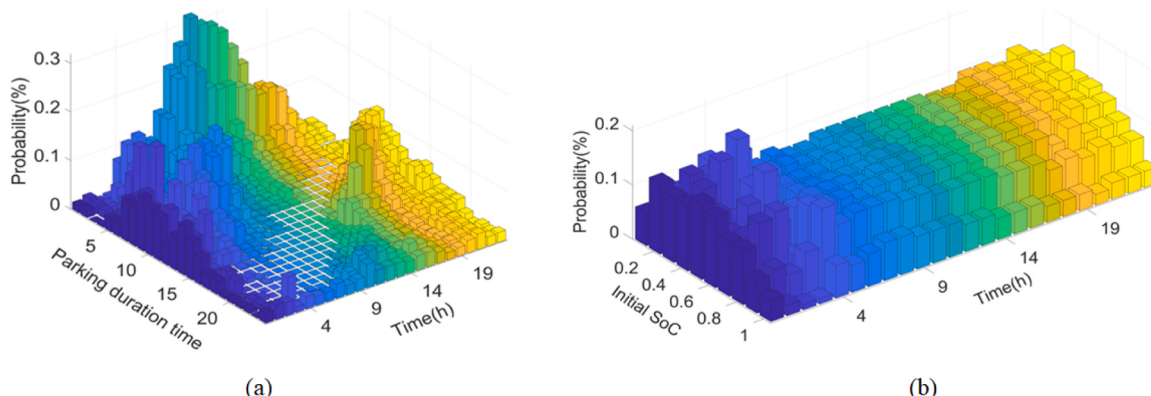


Fig. 7. (a) Hourly parking duration time probability mass function and (b) hourly initial state-of-charge probability mass function.

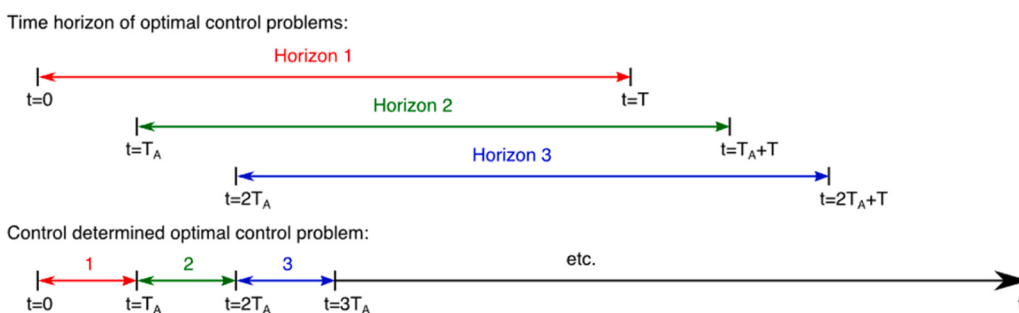


Fig. 8. Schematic diagram of the receding horizon control approach (Shapiro et al., 2017).

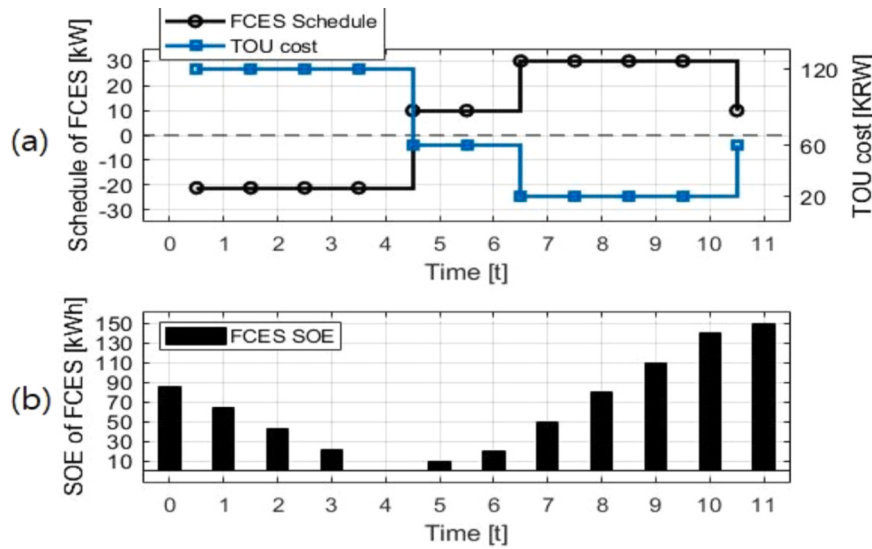


Fig. 9. (a) Schedule of the fictitious clustered energy storage (FCES) obtained in Stage A for Table 2 and (b) state of energy for the FCES according to its schedule.

adjusted, the amount of FCES discharge (85 kWh) during the on-peak hours ($t = 1\text{--}4$ h) could not be achieved (Fig. 10(b)), as the discharge limit of each EV was 10 kW while the initial charge of the EV3 was only 5 kWh. Subsequently, a non-feasible flag was presented in Stage B, and the ICUI method was applied, as shown in Fig. 5. The relaxed Stage B was re-performed using the ICUI method to detect the point at which capacity was violated. New constraints were then incrementally added to Stage B to curb the violations that occurred during the optimization. This process was repeated until Stage B became intractable. Then, the critical constraint was updated in Stage A.

The optimization results for Stage B before intractability was reached are presented in Table 3. The capacity violation at $t = 5$ and -10 kWh could be considered a primary factor that rendered the problem intractable. Therefore, a new constraint inhibiting the amount of charge before the time of the violation, $t = 5$, by 10 kWh was added to Stage A, as in (21). The entire optimization procedure was then iterated until Stage A generated a tractable FCES schedule for Stage B. The FCES schedule (black line) obtained from Stage A using the ICUI

method is shown in Fig. 11(a). Meanwhile, the TOU price is indicated

Table 3

Final tractable solution in the incremental constraint update and iteration Phase (B).

Charging (+)/discharging (-) power of the EVs

	$t = 1$	$t = 2$	$t = 3$	$t = 4$	$t = 5$
EV1	-10	-10	-10	-10	
EV2	-10	-10	-10	-10	
EV3	-1.25	-1.25	-1.25	-1.25	
SOE of the EVs					
EV1	50	40	30	20	10
EV2	30	20	10	0	-10
EV3	5	3.75	2.5	1.25	0

by the blue line, and the orange line is similar to that from the FCES schedule shown in Fig. 9(a). Fig. 11(b) shows the expected SOE according to each FCES schedule. The expected SOE of the re-obtained FCES schedule at $t = 4$ was not completely depleted as before. Fig. 12 (a) shows the re-obtained FCES schedule from Fig. 11 with each EV

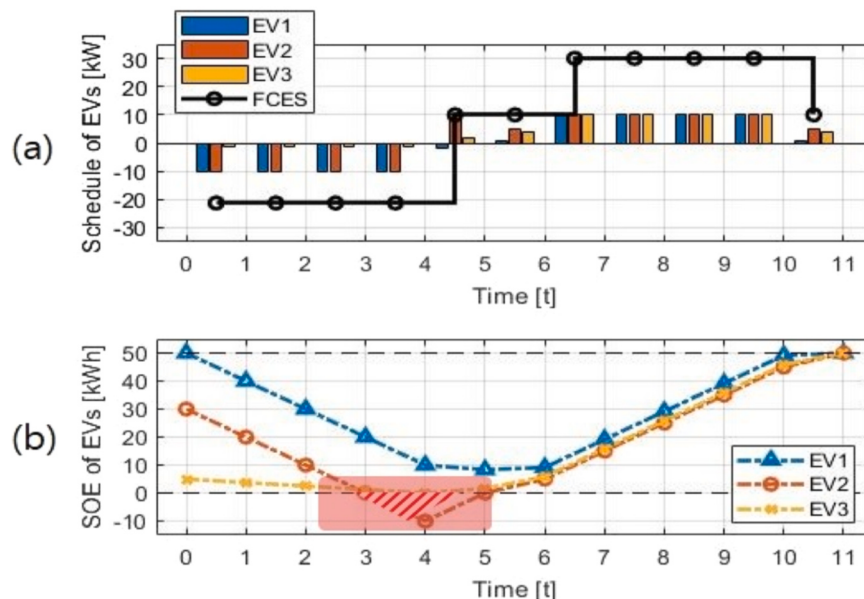


Fig. 10. (a) Schedule of each electric vehicle (EV) obtained in Stage B for Table 2 and (b) state of energy for each EV according to its schedule.

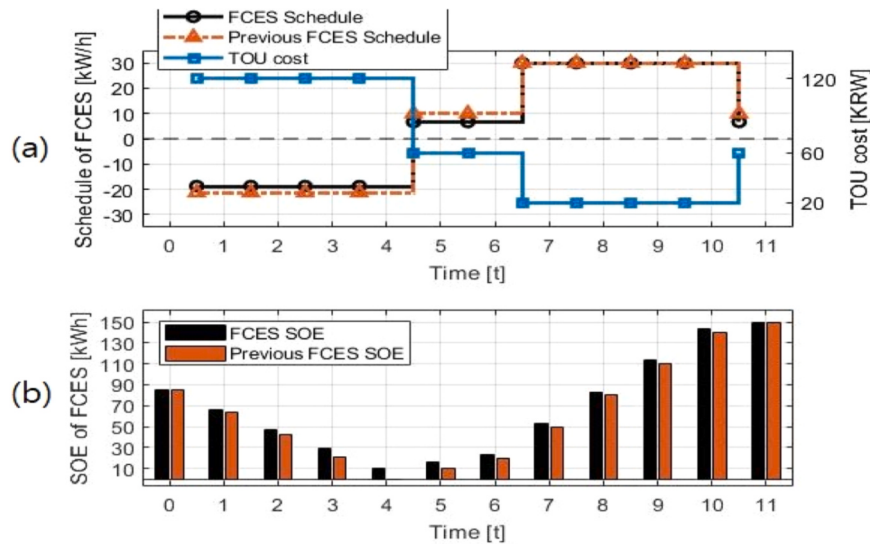


Fig. 11. (a) Schedule of the fictitious clustered energy storage (FCES) re-obtained in Stage A with strengthened constraints for Table 2 and (b) state of energy for the FCES according to its re-obtained schedule.

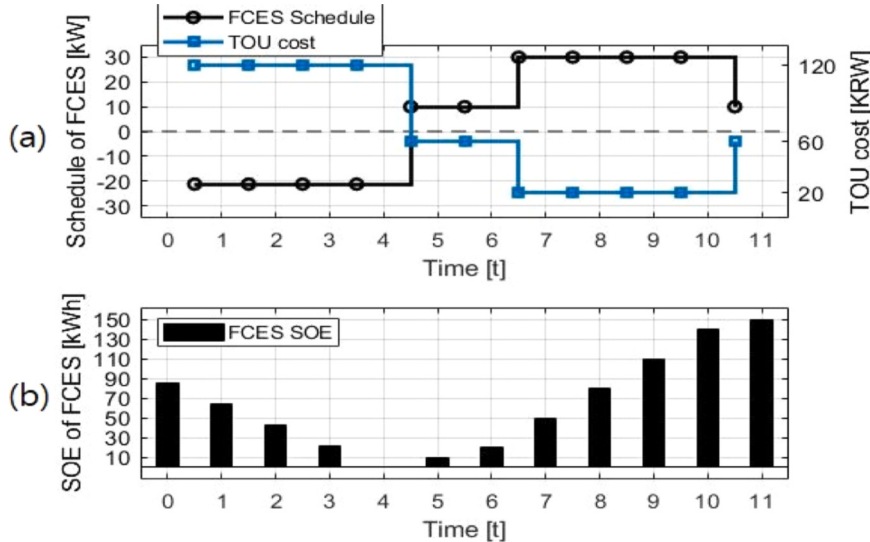


Fig. 12. (a) Schedule of each electric vehicle (EV) obtained in Stage B (from the re-obtained fictitious clustered energy storage schedule) for Table 2 and (b) state of energy for each EV according to its schedule.

schedule in which the FCES schedule was dispatched. The expected SOE for each EV according to the schedule for each EV dispatched is depicted in Fig. 12(b).

3.2. Case 2: comparison with a state-of-the-art scheduling method

In this section, the proposed methodology is compared with a state-of-the-art method (Sepetanc and Pandzic, 2021). According to Sepetanc and Pandzic (2021), a cluster-based scheduler (CBS) uses a clustering technique in which EVs are clustered into predetermined SOC levels. As a determinant, the CBS optimizes the number of EVs moving between predefined SOC clusters over time. Charging indicates a move to a SOC cluster higher than the current SOC level, whereas a move to a lower SOC level indicates discharging. The possible movement

$$\sum_{\text{idx}=1}^4 P_{1,\text{idx}} \leq \sum_{\text{idx}=1}^4 \text{preP}_{1,\text{idx}} - 10 \quad (21)$$

interval between clusters was set based on the physical constraints of the

EV and EVCS configurations. To the best of our knowledge, Sepetanc and Pandzic (2021) is the only published study in which the dispatching phase contains no missing order. However, only EVs with identical battery capacities and PCS outputs were clustered. Additionally, during the clustering process, the arrival and departure information for each vehicle were omitted; therefore, the charging requirement may not be met.

For example, the EV charging demands from a previous study were

Table 4
Electric vehicle configuration for Case 2.

Parameters	EV1	EV2	EV3
Battery capacity [kWh]	100	100	100
Initial energy [kWh]	30	70	80
Target SOE [kWh]	50	50	50
Charge/Discharge power limit [kW/h]	10/-10	10/-10	10/-10
Plug-time	1-3	1-8	1-9

modified, as shown in Table 4. The results of CBS scheduling for Table 4 are shown in Fig. 13. Predetermined SOC levels were set at 10 % intervals, and up to one space could be moved left and right in a single timeframe. The TOU was applied at $t = 1\text{--}2$ mid-peak, $t = 3\text{--}5$ on-peak, and $t = 6\text{--}9$ off-peak, such that the EV discharging and charging were set at $t = 1\text{--}5$ and $t = 6\text{--}9$, respectively, achieving the charge requirements. Because the EV arrival and departure information were omitted in the CBS cluster, the departure times of each EV were changed and scheduled. As in Fig. 10, the CBS/ICUI schedule with the dispatching result for each EV schedule (blue, orange, and yellow) is shown in Figs. 14(a) and 15(a). The expected SOE of each EV according to the schedule is shown in part (b) of the respective figures. EV1 in Fig. 14(b), that is, the plug-out SOE, was reduced compared with the plug-in SOC. Conversely, the target SOC level was achieved by the ICUI for all vehicles.

3.3. Verification of performance and optimality

Although both the ICUI and BAM produced the same schedule as in the previous section, the same outcome was not always guaranteed for the ICUI as for the BAM. The ICUI typically produced the same result as the BAM for small-scale problems. However, as the size of the problem grew, slightly poorer results occurred in terms of the cost optimization. The computation time of the ICUI was still considerably shorter than that of the BAM. To confirm this, simulations were performed using MATLAB R2021b on an Intel Core i5–6600 with a 3.30 GHz CPU and 16 GB of memory while the number of EVs was varied. The EV fleet data for the simulation were randomly generated using historical data from the PMF of the plug-in time, charge duration, and initial SOC provided by the FHWA. The PMF for EV charging behavior generated from data acquired from the FHWA was adopted from a previous study (Jin et al., 2020).

The number of ICUI iterations is shown in Fig. 16. An increase in the number of iterations could not be avoided, as the number of EVs increased. However, convergence was reached on the scheduling horizon. A comparison of the computation times of these methods is shown in Fig. 17. The computation time of the BAM increased exponentially as the number of EVs increased, whereas that of the ICUI remained comparably small and linear. The BAM simulation could not be performed with more than 1000 EVs because the required memory was greater than the available environment. The extrapolation curve (black-dashed line) was created for comparison with the ICUI. The declared decision variable was not correlated with the number of EVs, and iteration was not required for the CBS. The dispatching cluster schedule for

individual EVs was also included in the computation time; therefore, the computation time linearly increased as the number of EVs increased. The satisfaction ratio for the charging requirements of the ICUI and CBS is shown in Fig. 18. The limitation in Case 2 resulted in an average CBS satisfaction rate of approximately 64 %. Conversely, an average of approximately 94 % was realized for the ICUI. A comparison of the aggregation costs of the three methods (BAM, ICUI, and CBS) is shown in Fig. 19. All values were normalized because the resulting cost varied for the different EV sizes. In all cases, the cost of the ICUI was slightly higher (<5 %) than that of the BAM. The cost of the CBS was approximately 20–25 % higher than that of the BAM because of the less flexible control unit compared with that of the BAM and ICUI. The CBS is a low-complexity methodology that does not generate missing orders but has limitations in terms of cost optimization and satisfying charging requirements.

The case study depicted in Figs. 20 and 21 explores the stability of dynamic pricing by analyzing three models: a proposed model, the Deep Q-Network (DQN), and the Proximal Policy Optimization (PPO). Prior to presenting the results, it is essential to note the established research on these models. The PPO model, which employs a policy gradient approach for reinforcement learning, has been specifically noted for its efficacy in optimizing bidding strategies within the realms of energy and frequency regulation markets, as elaborated by (Anwar et al., 2022; Huang and Wang, 2021). This model's ability to take larger, more stable update steps is central to its application in such complex environments. In parallel, the stability of the Deep Q-Network (DQN) model in dynamic pricing scenarios is a hallmark of its design, merging Q-learning principles with deep neural networks to foster improved decision-making over discrete action spaces. The robustness and convergence of the DQN model in such fluctuating market conditions are noted feature in the works of (Chen et al., 2021; Wang et al., 2021). These models are evaluated based on their scheduling strategies for EV charging and discharging. Fig. 20 presents the 2022 day-ahead Locational Marginal Pricing (LMP) alongside the real-time LMP from PJM, which were employed to determine the models' performance. Scheduling and pricing decisions were based on the day-ahead LMP, while the real-time LMP was used to recalibrate the schedules, allowing for an assessment of the variance between predicted and actual prices. A deviation of approximately 19 % from the predicted LMP was observed, with sporadic occurrences of significant price fluctuations.

Fig. 21 furthers this examination, featuring a histogram (21(a)) and boxplot (21(b)) that detail the energy prices set by each model under both day-ahead and real-time LMP conditions. Blue denotes the

Time \ Cluster	10%	20%	30%	40%	50%	60%	70%	80%
	EV1; In						EV2; In	EV3; In
0	0	0	1	0	0	0	1	1
1	0	1	0	0	0	1	1	0
2	1	0	0	0	1	1	0	0
3	1	0	0	1	1	0	0	0
4	1	0	1	0	0	EV1; Out	0	0
5	1	1	0	0	0	0	0	0
6	0	1	1	0	0	0	0	0
7	0	0	1	1	0	EV2; Out	0	0
8	0	0	0	1	1	0	0	0
9	0	0	0	0	1	EV3; Out	0	0

Fig. 13. Scheduling results for the cluster-based scheduler in Sepetanc and Pandzic (2021).

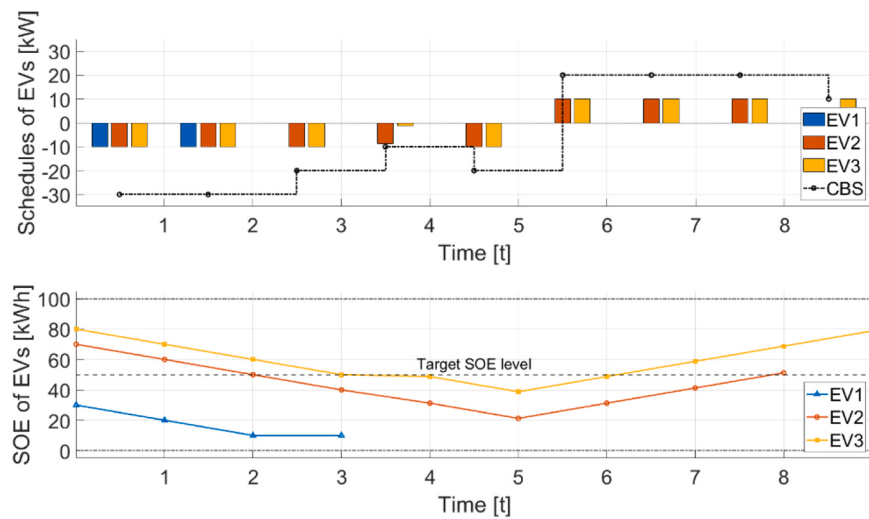


Fig. 14. (a) Dispatched schedule for each electric vehicle (EV) from the cluster-based scheduler for Table 4 and (b) state of energy for each EV according to its schedule.

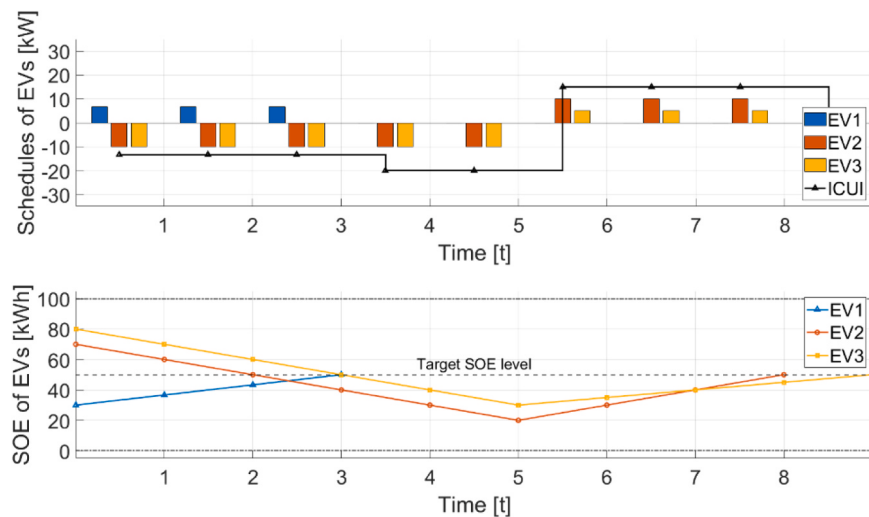


Fig. 15. (a) Dispatched schedule of each electric vehicle (EV) from the incremental constraint update and iteration for Table 4 and (b) state of energy for each EV according to its schedule.

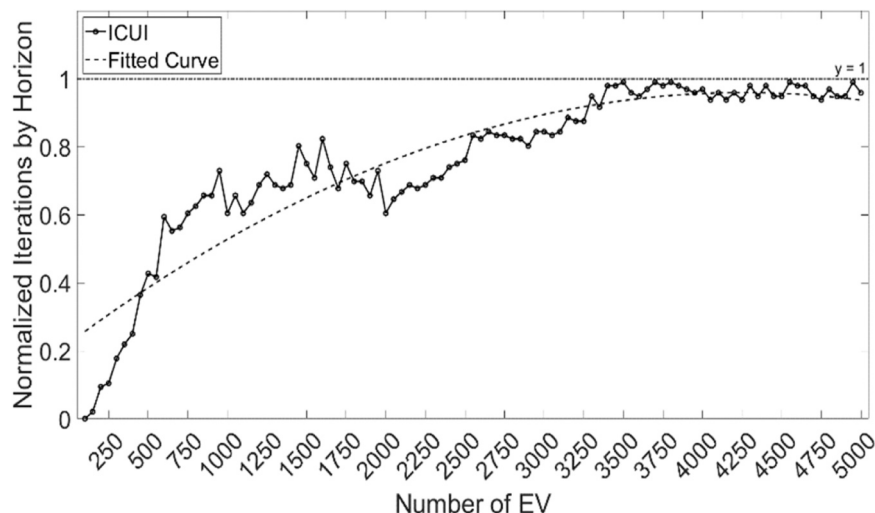


Fig. 16. Convergence of the proposed incremental constraint update and iteration (ICUI).

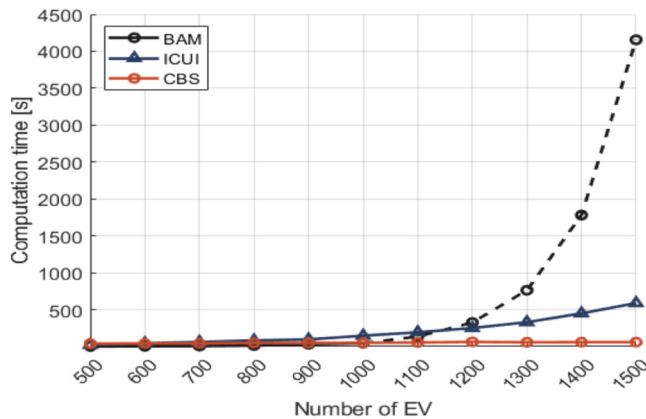


Fig. 17. Comparison of the computation time.

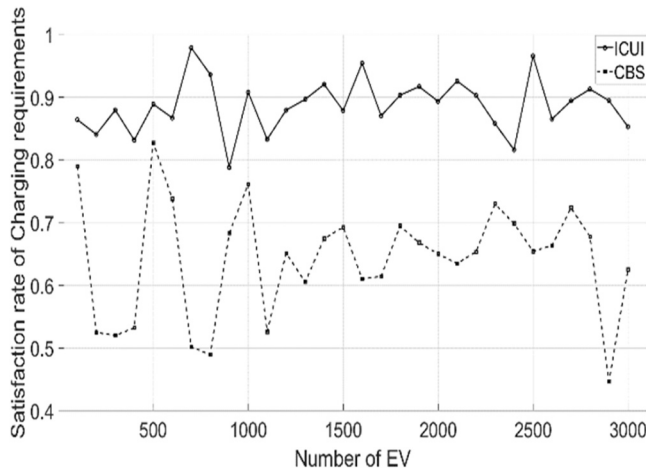


Fig. 18. Ratio of satisfaction for charging requirements.

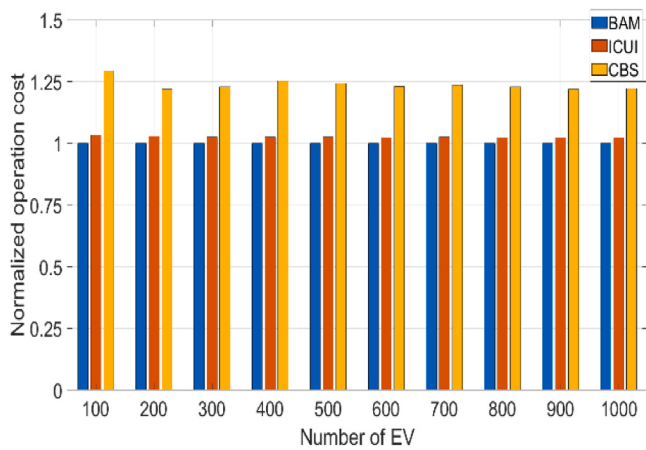


Fig. 19. Comparison of the aggregation costs.

Proposed model, red signifies the DQN, and green indicates the PPO. The histogram's mean and median are represented by colored dotted and dashed lines, respectively, while the boxplot's dotted lines depict the interquartile range for each model. Subsequently, the results of the models in this case study are presented. The effectiveness of the PPO model in the context of dynamic pricing is well-documented, and our analysis aligns with the aforementioned research, showing that the PPO model maintains a price variance of just 5 %, with a 95 % probability of

staying within this range. In contrast, the DQN model's stability in dynamic pricing has been confirmed through our findings, maintaining a price difference of 13 %. The proposed model, employing a convex optimization solver, exhibits a 15 % price difference. The potential of these reinforcement learning models is highlighted in dynamic pricing environments, which are commonly encountered in real-world scenarios such as EV charging and discharging schedules, with PPO being superior in terms of price optimization.

While reinforcement learning is known for its adaptability, it also incurs significant costs, which can be prohibitive in contexts such as V2G applications where the trial-and-error process is costly. Particularly at the point of service application, the absence of sufficient data for learning exacerbates these costs, making reinforcement learning less practical in the current V2G landscape. Conversely, mathematical models are superior in environments where model accuracy is high and uncertainty is low. Amid uncertainty, mathematical models can exploit robust control techniques for effective response (Cao et al., 2020; Tan et al., 2022). Thus, when the target application is a simplistic market and the prediction accuracy is guaranteed above a certain threshold, a mathematical model approach appears beneficial. However, it is crucial to recognize the intricate nature of the decision-making process when juxtaposing mathematical models with reinforcement learning. In markets characterized by high volatility and abundant data, reinforcement learning might be an indispensable asset. Conversely, in scenarios in which empirical data for an industry application remain limited, the deployment of a reinforcement learning strategy might be challenging until a sufficient amount of data is amassed. In such instances, an approach utilizing a mathematical model could offer a strategic advantage. Nonetheless, it is conceivable that with the exponential growth in data availability in future contexts, the potential of reinforcement learning as a disruptive force in various sectors could become increasingly prominent."

Finally, the EV SOC values were plotted in a three-dimensional histogram to investigate the capacity violations. Although the schedule was produced every 15 min, the values were clustered every 3 h to improve visibility. A 3-D histogram representing the expected SOC histogram based on the times of all EVs according to the derived schedule is shown in Fig. 22. The simulation results from a single run for 1000 EVs without the use of the ICUI scheme are presented. The expected SOC violations owing to the omission of individual EVs in the grouping process are marked with red-dotted lines, as shown in Fig. 10(b). Capacity violations were observed over the entire scheduling period. The expected SOC histogram of each EV derived by applying the ICUI scheme to the critical constraints in Fig. 22 is shown in Fig. 23. Conversely, the ICUI results in Fig. 23 demonstrate the lack of violations throughout the scheduling period, demonstrating the efficacy of the solution.

4. Conclusions and future work

In this study, an innovative technique for integrating EVs into the V2G concept is introduced, with a primary focus on addressing and rectifying overlooked constraints (missing order) in incorporating multiple EVs into a FCES. To maintain the integrity of optimization while reducing the problem size, an iterative multi-stage optimization method is presented, consisting of an EACM, multi-tier optimization model, and recursive framework. This method is particularly effective for massive EV fleets, offering optimal charge and discharge schedules for each vehicle while preserving high precision. Three illustrative examples, based on historical data provided by the FHWA, are presented to elucidate the logic behind the proposed model. Simultaneously, the effectiveness of the technique is validated through a progressive explanation. The energy expenditure of the introduced ICUI approach was demonstrated to be nearly identical to the global optimal solution, with an approximate difference of 4 % when compared with the BAM model. Through detailed simulations, the superior performance of the proposed model over pre-existing methods was confirmed. A noteworthy

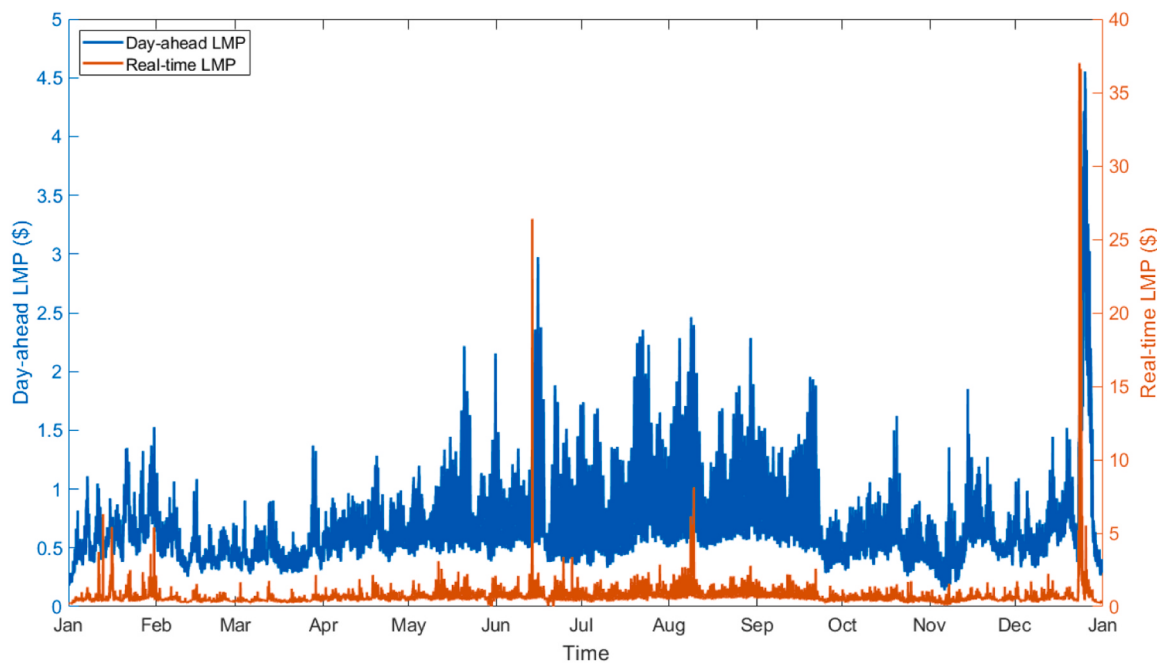


Fig. 20. Yearly comparison of day-ahead and real-time locational marginal price (2022, PJM).

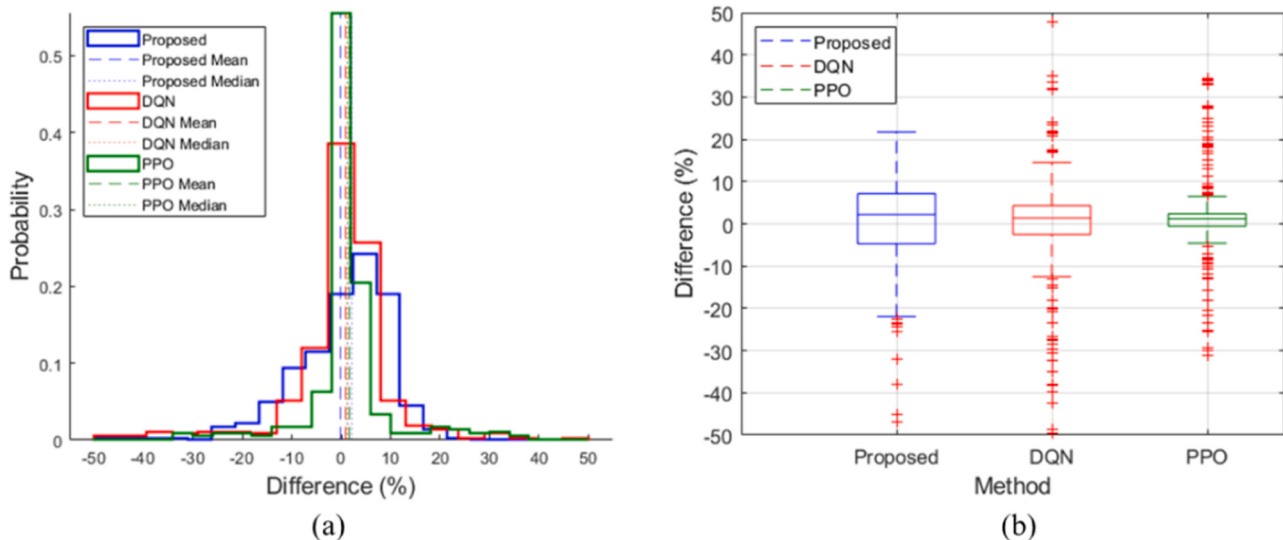


Fig. 21. Distribution and variance of fixed vs. dynamic pricing in scheduling models: (a) histogram, (b) boxplot.

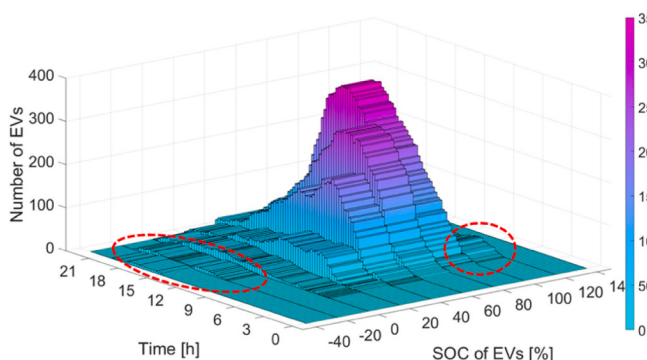


Fig. 22. Three-dimensional histogram of the state-of-charge of the electric vehicles fleet with a single dispatch in Stage B.

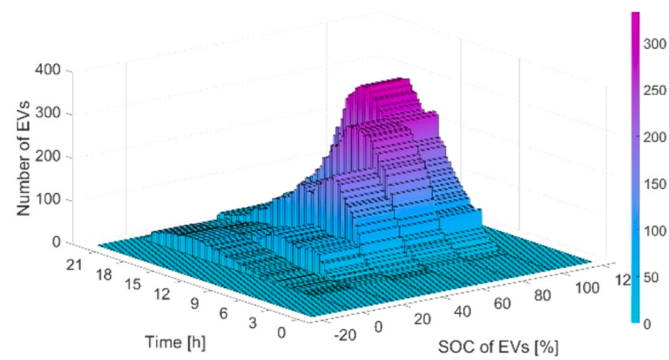


Fig. 23. Three-dimensional histogram of the state-of-charge of the electric vehicles fleet with incremental constraint update and iteration (ICUI).

observation from this study was the consistent computation time, regardless of the number of EVs, implying that the method is efficient in scaling without the manifestation of an upsurge in computation time. Furthermore, the model showed considerable resilience, enduring a moderate price differential of roughly 15 % under dynamic pricing circumstances, indicating its practical applicability.

However, despite the introduction of this novel and efficient approach for V2G integration, several potential areas of exploration for future research remain to augment the robustness and applicability of the proposed method. One pivotal area of focus involves the consideration of external influences such as battery degradation and driver behavior. Future research is necessary to integrate battery degradation models into V2G aggregation methodologies, analyzing the substantial effect of battery degradation on the performance and longevity of EVs. This would enable a more precise representation of EV performance over time. Driver behavior is another essential factor influencing the charge and discharge schedules of EVs. Future research should consider individual driving patterns and preferences in optimization models, which could involve the construction of driver behavior predictive models from historical data or the use of surveys to collect data on driver preferences and habits. Moreover, general strategies should be derived for equilibrating the market on a broader EV scale. Such strategies could encompass various market rules, such as compensation, unit allocation, and lead times for customer baseload lines. Then, the strategies could be empirically tested using an agent-based demonstration platform involving multiple energy aggregators offering demand response. This platform would provide an avenue for refining the developed model, allowing for a deeper understanding of the benefits of centralized control over large EV fleets.

CRediT authorship contribution statement

Seo Mingyu: Conceptualization, Formal analysis, Investigation, Methodology, Software, Visualization, Writing – original draft. **Kodaira Daisuke:** Project administration. **Jin Yuwei:** Visualization, Writing – review & editing. **Son Hyeongyu:** Resources. **Han Sekyung:** Supervision, Writing – review & editing.

Declaration of Competing Interest

The authors declare the following financial interests/personal relationships which may be considered as potential competing interests: Sekyung Han reports financial support was provided by Korea Electrotechnology Research Institute and Korea Institute of Energy Technology Evaluation and Planning.

Data Availability

The authors do not have permission to share data.

Acknowledgements

This research was supported by Korea Electrotechnology Research Institute (KERI) Primary research program through the National Research Council of Science & Technology (NST) funded by the Ministry of Science and ICT (MSIT) (No. 23A01069).

This work was supported by the Human Resources Program in Energy Technology of the Korea Institute of Energy Technology Evaluation and Planning(KETEP) granted financial resource from the Ministry of Trade, Industry & Energy, Republic of Korea (No. 20204010600060).

References

- Alghamdi, T.G., Said, D., Moutah, H.T., 2020. Decentralized game-theoretic scheme for D-EVSE based on renewable energy in smart cities: a realistic scenario. *IEEE Access* 8, 48274–48284.
- Anwar, M., Wang, C., de Nijs, F., & Wang, H. (2022). Proximal Policy Optimization Based Reinforcement Learning for Joint Bidding in Energy and Frequency Regulation Markets. <https://doi.org/10.1109/PESGM48719.2022.9917082>.
- Arias, N.B., Hashemi, S., Andersen, P.B., Traholt, C., Romero, R., 2018. V2G enabled EVs providing frequency containment reserves: field results. *Proc. IEEE Int. Conf. Ind. Technol.* 1814–1819, 2018–Febru.
- Cao, Y., Huang, L., Li, Y., Jermittiparsert, K., Ahmadi-Nezamabad, H., Nojavan, S., 2020. Optimal scheduling of electric vehicles aggregator under market price uncertainty using robust optimization technique. *Int. J. Electr. Power Energy Syst.* 117.
- Chen, S.J., Chiu, W.Y., Liu, W.J., 2021. User preference-based demand response for smart home energy management using multiobjective reinforcement learning. *IEEE Access* 9, 161627–161637.
- Diaz-Londono, C., Ruiz, F., Mazza, A., Chicco, G., 2020. Optimal operation strategy for electric vehicles charging stations with renewable energy integration. *IFAC-Pap.* 53, 12739–12744.
- Dik, A., Omer S., Bouhanouf R. 2022. Electric Vehicles: V2G for Rapid, Safe, and Green EV Penetration.
- Domínguez-Navarro, J.A., Dufo-López, R., Yusta-Loyo, J.M., Artal-Sevil, J.S., Bernal-Agustín, J.L., 2019. Design of an electric vehicle fast-charging station with integration of renewable energy and storage systems. *Int. J. Electr. Power Energy Syst.* 105 (March 2018), 46–58.
- Duran, M.A., Grossmann, I.E., 1986. An outer-approximation algorithm for a class of mixed-integer nonlinear programs. *Math. Program* 36 (3), 307–339.
- Einaddin, A.H., Yazdankhah, A.S., 2020. A novel approach for multi-objective optimal scheduling of large-scale EV fleets in a smart distribution grid considering realistic and stochastic modeling framework. *Int. J. Electr. Power Energy Syst.* 117.
- Electric Rates Table | KEPCO. (<http://cyber.kepc.co.kr>).
- Farhat, M., Kamel, S., Atallah, A.M., Khan, B., 2021. Optimal power flow solution based on jellyfish search optimization considering uncertainty of renewable energy sources. *IEEE Access* 9, 100911–100933.
- Hashemipour, N., Crespo del Granado, P., Aghaei, J., 2021. Dynamic allocation of peer-to-peer clusters in virtual local electricity markets: a marketplace for EV flexibility. *Energy* 236.
- Huang, B., Wang, J., 2021. Deep-reinforcement-learning-based capacity scheduling for PV-battery storage system. *IEEE Trans. Smart Grid* 12 (3), 2272–2283. <https://doi.org/10.1109/TSG.2020.3047890>.
- Jin, Y., Yu, B., Seo, M., Han, S., 2020. Optimal aggregation design for massive V2G participation in energy market. *IEEE Access* 8, 211794–211808.
- Kandpal, B., Pareek, P., Verma, A., 2022. A robust day-ahead scheduling strategy for EV charging stations in unbalanced distribution grid. *Energy* 249.
- Karthik T., Prathyusha M., Thirumalaiwasan R., Janaki M. 2019. Power quality improvement using DSTATCOM. 2019 Innovations in Power and Advanced Computing Technologies, i-PACT 2019. 311–16.
- Khalil, A., Alfergani, A., Shaltami, F.M., Asheibi, A., 2023. Robust stabilization of a microgrid with communication delay and uncertainties. *Computation* 11 (4).
- Khan, M.M.H., Hossain, A., Ullah, A., Lipu, M.S.H., Shahnewaz Siddiquee, S.M., et al., 2021. Integration of large-scale electric vehicles into utility grid: an efficient approach for impact analysis and power quality assessment. *Sustain. (Switz.)* 13 (19).
- Khan, S.U., Mehmood, K.K., Haider, Z.M., Bukhari, S.B.A., Lee, S.J., et al., 2018. Energy management scheme for an EV smart charger V2G/G2V application with an EV power allocation technique and voltage regulation. *Appl. Sci. (Switz.)* 8 (4).
- Li, X., Wang, Z., Zhang, L., Sun, F., Cui, D., et al., 2023. Electric vehicle behavior modeling and applications in vehicle-grid integration: an overview. *Energy* 268.
- Liang, H., Liu, Y., Li, F., Shen, Y., 2019. Dynamic economic/emission dispatch including PEVs for peak shaving and valley filling. *IEEE Trans. Ind. Electron.* 66 (4), 2880–2890.
- Lopez, K.L., Gagne, C., Gardner, M.A., 2019. Demand-side management using deep learning for smart charging of electric vehicles. *IEEE Trans. Smart Grid* 10 (3), 2683–2691.
- Park, K., Moon, I., 2022. Multi-agent deep reinforcement learning approach for EV charging scheduling in a smart grid. *Appl. Energy* 328.
- Patil H., Kalkhambkar V.N. 2021. Grid Integration of Electric Vehicles for Economic Benefits: A Review.
- Paudel, A., Hussain, S.A., Sadiq, R., Zareipour, H., Hewage, K., 2022. Decentralized cooperative approach for electric vehicle charging. *J. Clean. Prod.* 364.
- Qiu, Y.L., Wang, Y.D., Iseki, H., Shen, X., Xing, B., Zhang, H., 2022. Empirical grid impact of in-home electric vehicle charging differs from predictions. *Resour. Energy Econ.* 67.
- Rezaeimozafar, M., Eskandari, M., Savkin, A. v., 2021. A self-optimizing scheduling model for large-scale EV fleets in microgrids. *IEEE Trans. Ind. Inf.*
- Sepetanc, K., Pandzic, H., 2021. A cluster-based model for charging a single-depot fleet of electric vehicles. *IEEE Trans. Smart Grid* 12 (4), 3339–3352.
- Shapiro, C.R., Bauweraerts, P., Meyers, J., Meneveau, C., Gayme, D.F., 2017. Model-based receding horizon control of wind farms for secondary frequency regulation. *Wind Energy* 20 (7), 1261–1275.
- Tan, B., Chen, H., Zheng, X., Huang, J., 2022. Two-stage robust optimization dispatch for multiple microgrids with electric vehicle loads based on a novel data-driven uncertainty set. *Int. J. Electr. Power Energy Syst.* 134.
- Wang, L., Sharkh, S., Chipperfield, A., 2018. Optimal decentralized coordination of electric vehicles and renewable generators in a distribution network using A* search. *Int. J. Electr. Power Energy Syst.* 98, 474–487.
- Wang, R., Wang, P., Xiao, G., 2016. Two-stage mechanism for massive electric vehicle charging involving renewable energy. *IEEE Trans. Veh. Technol.* 65 (6), 4159–4171.

- Wang, R., Xiao, G., Wang, P., 2017. Hybrid centralized-decentralized (HCD) charging control of electric vehicles. *IEEE Trans. Veh. Technol.* 66 (8), 6728–6741.
- Wang, X., Wang, J., Liu, J., 2021. Vehicle to grid frequency regulation capacity optimal scheduling for battery swapping station using deep Q-network. *IEEE Trans. Ind. Inf.* 17 (2), 1342–1351.
- Wang, Z., Jochem, P., Fichtner, W., 2020. A scenario-based stochastic optimization model for charging scheduling of electric vehicles under uncertainties of vehicle availability and charging demand. *J. Clean. Prod.* 254.
- Wu, F., Sioshansi, R., 2017. A two-stage stochastic optimization model for scheduling electric vehicle charging loads to relieve distribution-system constraints. *Transp. Res. Part B: Methodol.* 102, 55–82.
- Yusuf J., Hasan A.S.M.J., Ula S. 2021. Impacts Analysis Field Implementation of Plug-in Electric Vehicles Participation in Demand Response and Critical Peak Pricing for Commercial Buildings. 2021 IEEE Texas Power and Energy Conference, TPEC 2021. Institute of Electrical and Electronics Engineers Inc.
- Zhao T., Li Y., Pan X., Wang P., Zhang J. 2018. Real-Time Optimal Energy and Reserve Management of Electric Vehicle Fast Charging Station: Hierarchical Game Approach. *IEEE Trans Smart Grid.* 9(5):5357–5370.
- Zhaoan, F., Baochuan, F., Xuefeng, X., Zhengtian, W., Zhenping, C., Xinyin, X., 2020. Power charging management strategy for electric vehicles based on a Stackelberg game. *IET Intell. Transp. Syst.* 14 (5), 432–439.